

Structure–Function Analysis of RAMP1 by Alanine Mutagenesis<sup>†</sup>John Simms,<sup>‡,§,||</sup> Debbie L. Hay,<sup>‡,⊥</sup> Richard J. Bailey,<sup>⊥</sup> Galina Konycheva,<sup>⊥</sup> Graham Bailey,<sup>⊥</sup> Mark Wheatley,<sup>#</sup> and David R. Poyner<sup>\*,§</sup>*School of Life and Health Sciences, Aston University, Birmingham B4 7ET, U.K., Department of Pharmacology, University of Monash, Clayton 3800, Australia, School of Biological Sciences, University of Auckland, Auckland, New Zealand, and School of Biosciences, University of Birmingham, Birmingham B15 2TT, U.K.**Received October 3, 2008; Revised Manuscript Received November 19, 2008*

**ABSTRACT:** Receptor activity modifying protein 1 (RAMP1) is an integral component of several receptors including the calcitonin gene-related peptide (CGRP) receptor. It forms a complex with the calcitonin receptor-like receptor (CLR) and is required for receptor trafficking and ligand binding. The N-terminus of RAMP1 comprises three helices. The current study investigated regions of RAMP1 important for CGRP or CLR interactions by alanine mutagenesis. Modeling suggested the second and third helices were important in protein–protein interactions. Most of the conserved residues in the N-terminus (M48, W56, Y66, P85, N66, H97, F101, D113, P114, P115), together with a further 13 residues spread throughout three helices of RAMP1, were mutated to alanine and coexpressed with CLR in Cos 7 cells. None of the mutations significantly reduced RAMP expression. Of the nine mutants from helix 1, only M48A had any effect, producing a modest reduction in trafficking of CLR to the cell surface. In helix 2 Y66A almost completely abolished CLR trafficking; L69A and T73A reduced the potency of CGRP to produce cAMP. In helix 3, H97A abolished CLR trafficking; P85A, N86A, and F101A had caused modest reductions in CLR trafficking and also reduced the potency of CGRP on cAMP production. F93A caused a modest reduction in CLR trafficking alone and L94A increased cAMP production. The data are consistent with a CLR recognition site particularly involving Y66 and H97, with lesser roles for adjacent residues in helix 3. L69 and T73 may contribute to a CGRP recognition site in helix 2 also involving nearby residues.

Receptor activity modifying proteins (RAMPs)<sup>1</sup> are a family of three single-pass transmembrane proteins that associate with certain G-protein coupled receptors (GPCR) (1). Their best studied actions are with the calcitonin receptor-like receptor (CLR). By itself this is only poorly expressed at the cell surface and interacts with no known ligand. However, when coexpressed with RAMP1, it forms a receptor for calcitonin gene-related peptide (CGRP), the CGRP receptor. In combination with RAMP2 or RAMP3 it forms two distinct receptors for adrenomedullin (AM), the AM<sub>1</sub> and AM<sub>2</sub> receptors (2). The three RAMPs can also interact with the calcitonin receptor, in each case producing

a receptor with high affinity for the peptide amylin (2, 3). Interactions with other family B GPCRs have also been described, as well as with the calcium sensing receptor, a family C GPCR (4–6).

Each of the three RAMPs has an N-terminal extracellular domain of around 100 amino acids. By contrast, the intracellular domain for each is only around 10 residues long. Thus, it is predicted that the extracellular domains of these proteins are crucial for their functions. This is supported experimentally in that chimeras have clearly established the significance of the N-termini of the RAMPs for ligand binding (7–9). The RAMPs presumably modify the conformation of the N-terminus of the GPCR and potentially influence ligand binding at this site (10). There are a number of conserved cysteines that are involved in disulfide bonds (11, 12). However, there is little information on the role of individual amino acids, and little work has been done to understand the detailed structure of RAMPs or to relate this to their pharmacological properties. A series of deletions and point mutations indicated that residues 91–103 contain amino acids which are required for high-affinity CGRP binding (13). It has also been shown that Trp-74 is required for binding of the nonpeptide antagonist BIBN4096BS to CGRP and amylin receptors (14–16); its equivalent in RAMP3 may be a contact point for adrenomedullin (15).

To help to understand the molecular basis for RAMP modulation of GPCR biology, we produced an *ab initio* model of the extracellular domain of human RAMP1 that predicted that it consisted of three helices (17). The major

<sup>†</sup> This work was supported by grants from the Biotechnology and Biological Sciences Research Council of the U.K. (C20090) to D.R.P. and M.W. D.L.H. was supported by the Auckland Medical Research Foundation, Maurice and Phyllis Paykel Trust, Health Research Council, and the New Zealand Lottery Health Fund.

\* To whom correspondence should be addressed. Tel: +44 (0)121 359 3611. Fax: +44 (0)121 359 5142. E-mail: D.R.Poyner@aston.ac.uk.

<sup>‡</sup> J.S. and D.L.H. were equal contributors to this study.

<sup>§</sup> Aston University.

<sup>||</sup> University of Monash.

<sup>⊥</sup> University of Auckland.

<sup>#</sup> University of Birmingham.

<sup>1</sup> Abbreviations: AM, adrenomedullin; BIBN4096BS, *N*-[2-[[5-amino-1-[[4-(4-pyridinyl)-1-piperazinyl]carbonyl]pentyl]amino]-1-[(3,5-dibromo-4-hydroxyphenyl)methyl]-2-oxoethyl]-4-(1,4-dihydro-2-oxo-3(2*H*)-quinazolinyl)-1-piperidinecarboxamide; CGRP, calcitonin gene-related peptide; CLR, calcitonin receptor-like receptor; *E*<sub>max</sub>, maximum response; GPCR, G-protein coupled receptor; HA, hemagglutinin; pEC<sub>50</sub>, –log(EC<sub>50</sub>); RAMP, receptor activity modifying protein; TBS, Tris-buffered saline; WT, wild type.

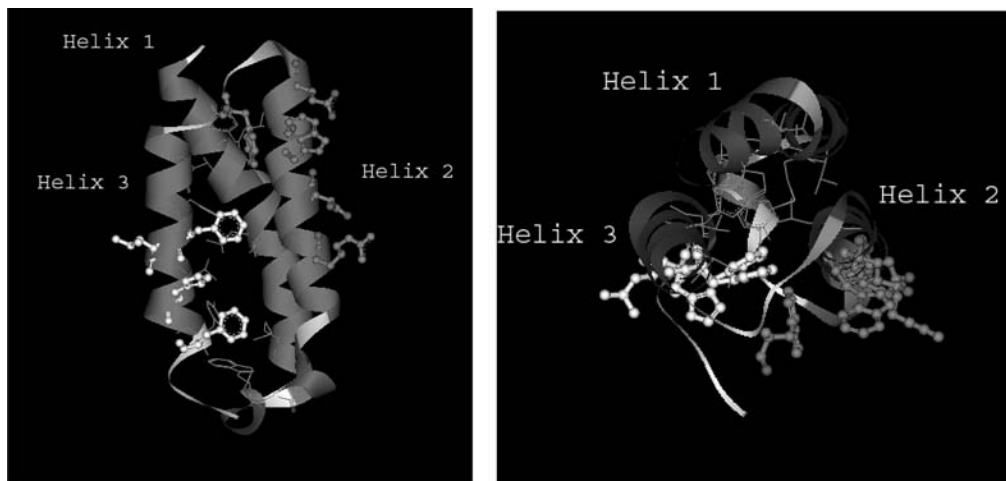


FIGURE 1: Crystal structure of the N-terminus of RAMP1. The structure is taken from Kusano et al. (18). Left, sideways view; right, top view. Residues shown in line form are important for interhelical packing; residues in gray ball and stick form are part of the proposed ligand binding pocket; residues in white ball and stick form are part of the proposed CLR interaction site.

features of this model have recently been confirmed and the details refined by a crystal structure of the isolated N-terminus of RAMP 1 (18). Although not tested experimentally, in that study, a hydrophobic patch at the C-terminal end of helix 3 was suggested as a CLR binding site, and a further cluster of residues at the N-terminal end of helix 2 was proposed to be involved in CGRP binding (Figure 1).

To further understand the structure–function relationship for RAMP1, we have carried out an alanine scan on the amino acids that are conserved in the N-terminus of all three human RAMPs. In addition, we have mutated a number of residues in other parts of the protein to help to define the role of its three helices, guided in part by protein–protein prediction algorithms. To study the pharmacological consequences of this, we have expressed the mutated receptors with CLR to give the CGRP receptor. The study demonstrates that mutation of residues in the predicted second and third helices frequently disrupts receptor function, whereas mutation of residues in the predicted first helix was largely without effect.

## EXPERIMENTAL PROCEDURES

**Materials.** Human  $\alpha$ CGRP and human AM were from Bachem (Bubendorf, Switzerland). Peptides were dissolved in distilled water and stored as aliquots at  $-20^{\circ}\text{C}$  in siliconized microcentrifuge tubes (Bio Plas). Unless otherwise specified, chemicals were from Sigma (St. Louis, MO). Cell culture reagents were from Invitrogen (Carlsbad, CA). Forskolin was from Tocris (Ellisville, MO).

**Expression Constructs and Mutagenesis.** Human CLR with an N-terminal hemagglutinin (HA) epitope tag (HA-CL) and human RAMP1 with or without a myc epitope tag (mycRAMP1) were provided by Dr. S. M. Foord (GlaxoWellcome, Stevenage, U.K.). RAMP1 was subcloned into pcDNA3.1(+) (Invitrogen) prior to mutagenesis. Mutagenesis was carried out using the QuikChange site-directed mutagenesis kit (Stratagene, Cambridge, U.K.), following the manufacturer's instructions. Forward and reverse oligonucleotide primers were designed with single base changes to incorporate amino acid point mutations and to engineer

restriction sites to aid screening of mutants in the final constructs as necessary. The primers were synthesized by Invitrogen.

Plasmid DNA was extracted from the cultures using a Wizard-Prep DNA extraction kit according to the manufacturer's instructions (Promega, Southampton, U.K.). The plasmid DNA was eluted in  $100\ \mu\text{L}$  of sterile distilled water and stored at  $-20^{\circ}\text{C}$ . Sequences were confirmed by sequencing (Functional Genomics, Birmingham, U.K., or School of Biological Sciences, University of Auckland, New Zealand).

**Cell Culture and Transfection.** Culture of Cos 7 cells was described previously (17). Cells were cultured in Dulbecco's modified Eagle's medium (DMEM) containing 8% heat-inactivated fetal bovine serum (FBS) and 5% (v/v) penicillin/streptomycin. Cells were plated into 96-well plates 1 day prior to transfection with polyethylenimine (PEI) as described (17). For preparation of cell lysates for Western blotting, cells were plated into 6-well plates and transfected with a total of  $5\ \mu\text{g}$  of DNA per well.

**Assay of cAMP Production.** Growth medium was removed from the cells and replaced with Dulbecco's modified Eagle's medium containing 1 mM isobutylmethylxanthine and 0.1% BSA for 30 min. Human  $\alpha$ CGRP in the range 1 pM to 1  $\mu\text{M}$  was added for a further 15 min. Ice-cold ethanol (95–100% v/v) was used to extract cAMP, which was subsequently measured by radio-receptor assay in a 96-well plate as previously described (19). A positive control of 50  $\mu\text{M}$  forskolin was included in every experiment, and cAMP was normalized to this as 100%.

**Analysis of Cell-Surface Expression of Mutants by ELISA.** Cell-surface expression of mutant receptor complexes was measured as previously described (20). Briefly, cells were fixed and then washed in phosphate-buffered saline (PBS) prior to incubation for 20 min in 0.6% hydrogen peroxide in PBS and blocked in 10% goat serum (in PBS) for 1 h. Cells were incubated with anti HA.11 monoclonal primary antibody (Covance: MMS-101P, diluted 1:2000 in PBS with 1% goat serum) for 30 min at  $37^{\circ}\text{C}$ . After one wash, horseradish peroxidase-linked anti-mouse secondary antibody (Amersham: NA931-1 ML, diluted 1:500 in PBS with 1%

goat serum) was added and incubated at room temperature for 1 h. After two washes in PBS, substrate (SIGMAFAST OPD (Sigma)) was added and incubated for 15 min in the dark. The reaction was terminated with 0.5 M H<sub>2</sub>SO<sub>4</sub>, and plates were read at A<sub>490</sub> and A<sub>650</sub>. After two washes, cresyl violet stain was added to each well for 30 min. The wells were washed once, and 1% SDS was added for 1 h. The A<sub>595</sub> was determined and the (A<sub>490</sub> - A<sub>650</sub>)/A<sub>595</sub> calculated for each well. Values were background-corrected and normalized to wild-type HA-CL/RAMP1 expression levels. The absorbance measured by the ELISA showed a linear dependence on the DNA concentration used in the transfection.

**Analysis of Total Mutant Expression by Western Blotting.** Cells in 6-well plates were washed with ice-cold PBS, scraped in 1.5 mL of ice-cold PBS, and collected in 1.5 mL microcentrifuge tubes. Cells were pelleted at 6000 rpm in a benchtop centrifuge for 5 min at 4 °C. The supernatant was discarded, and the cell pellet was resuspended in 60 µL of lysis buffer (1% (v/v) Triton X-100, 10% (v/v) glycerol, 150 mM NaCl, 20 mM Hepes (pH 7.5)) containing protease inhibitor cocktail (Sigma, P8340, 1:100 dilution). Cells were left on ice to lyse for 30 min and then spun at 10000 rpm for 10 min at 4 °C in a benchtop centrifuge. The supernatant was collected, and protein concentration was estimated using Quick Start Bradford Dye Reagent 1X protein measurement assay (Bio-Rad). Cell lysates were mixed with NuPAGE LDS sample buffer 4X (Invitrogen), containing 200 mM DTT, and heated at 90 °C for 5 min. Twenty micrograms of protein was applied to the NuPAGE 4–12% Bis-Tris pre-cast gel system (Invitrogen). The gels were electrophoresed at 200 V for 40 min, and proteins were transferred onto iBlot gel transfer stacks polyvinylidene fluoride (PVDF) membrane (Invitrogen) using the iBlot dry blotting system (Invitrogen) following the manufacturer's instructions. Blots were blocked with 10% goat serum in Tris-buffered saline (TBS, pH 7.4) containing 0.1% Tween20 (TBS-T) for 1 h at room temperature, followed by two 5 min washes in TBS-T. Blots were incubated overnight at 4 °C with 1:400 dilution of primary anti-c-Myc mouse mAb (9E10, Calbiochem) and an antibody specific for glyceraldehyde-3-phosphate dehydrogenase (GAPDH) at a dilution of 1:200000 (Abcam, 6C5, AB8245) prepared in TBS-T containing 2% of goat serum. The blots were then washed three times for 5 min each at room temperature with TBS-T and incubated for 1 h at room temperature with a 1:2000 dilution of secondary Ecl sheep anti-mouse horseradish peroxidase linked antibody (GE Healthcare) prepared in 10% goat serum in TBS-T. Blots were washed 4 times in TBS-T for 5 min and once with TBS for 5 min at room temperature. The PVDF membranes were developed with ECL Plus Western blotting detection system (Amersham) for 5 min, and the chemiluminescent signal was detected using LAS3000 imaging system (Fujifilm). Protein bands were analyzed densitometrically with Multi Gauge software v2.2 (Fujifilm). The intensity of each single band detected with the anti-c-Myc antibody was normalized to the intensity of corresponding GAPDH band from the same lane to account for possible differences in protein loading. Normalized protein band intensities were expressed as a percentage of the WT mycRAMP1/HA-CL control sample intensities. Three independent transfections were performed for each mutant and WT and run on independent gels.

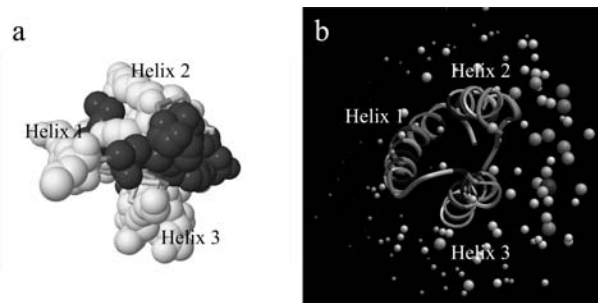


**FIGURE 2:** Predicted protein–protein interaction sites of RAMP1. (a) ConSurf representation of RAMP1. The image is shown in gray scale and the darker the molecular surface the higher score obtained under ConSurf. (b) ODA representation of RAMP1. This method shows the regions of favorable energy once buried at an interface; this is depicted as large spheres as seen in helices 2 and 3. In contrast, helix 1 is associated with an unfavorable buried energy and is depicted as small spheres. Both methods highlight the region between helices 2 and 3 as important in RAMP1 function.

**Prediction of the RAMP1 Interface.** The RAMP1 structure (2YX8) was submitted to the ConSurf server (21) (<http://consurf.tau.ac.il/>) to identify functionally important regions in the structure. The regions of conservation were then projected onto the molecular surface of RAMP1 and visualized using DEEVIEW. In addition, RAMP interaction surfaces were predicted using the ODA module as implemented in ICM (22).

**Data Analysis.** Curve fitting was done with PRISM 4 (Graphpad Software Inc., San Diego, CA). For cyclic AMP studies, the data from each concentration–response curve were fitted to a sigmoidal curve to obtain the maximum response ( $E_{\max}$ ) and  $-\log EC_{50}$  ( $pEC_{50}$ ). The  $E_{\max}$  was expressed as a percentage of the forskolin control.  $pEC_{50}$  and  $E_{\max}$  values were compared by Student's *t* test or by one-way ANOVA followed by Dunnett's test. A control WT experiment was included in every experiment.

## RESULTS

**Comparison of the RAMP Model with the Crystal Structure.** The newly available crystal structure for RAMP1 allows an assessment of the accuracy of our original *ab initio* model. The rmsd between the two structures is 2.20 Å for all Cα atoms including loop regions and 1.86 Å Cα RMSD for helical regions (Figures S1 and S2). Thus there is very good agreement between the two structures.

**Predicted Protein–Protein Interaction Sites.** The crystal structure of the N-terminus of RAMP1 was analyzed using two complementary methods that predict possible protein–protein interaction sites. The first of these, ConSurf, uses sequence-based conservation scores which are correlated with biological function, normally protein–protein interaction sites. This is in contrast to ODA (optimal docking area) which is a physical-based method that identifies areas with favorable energy change when buried as in protein–protein association. Comparison of both sets of data revealed a common predicted docking surface for RAMP1 which is located at the solvent-accessible interface between helices 2 and 3 (Figure 2). Several conserved residues are identified in this region; Y66, P85, N86, H97, and F101. This region also corresponds to the hydrophobic patch identified by Kusano et al. as a potential CLR interaction site and is adjacent to their



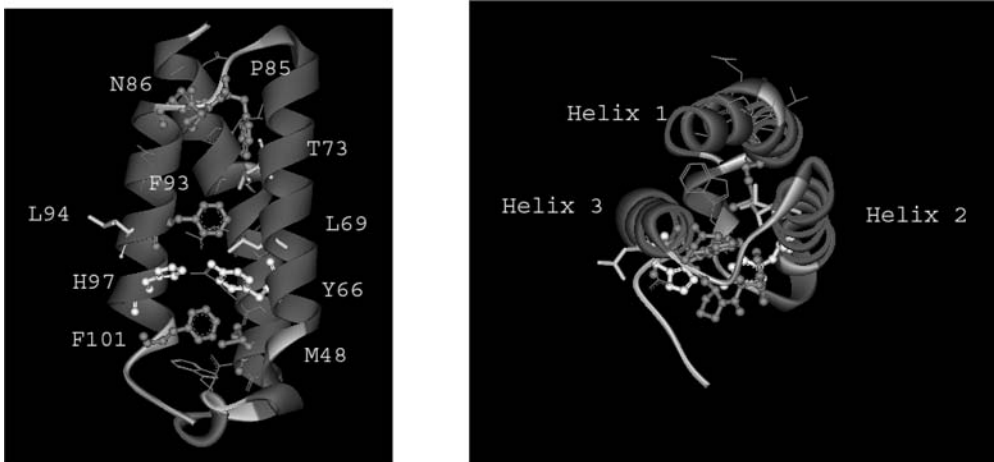


FIGURE 3: Location of mutated residues on RAMP1. Left, sideways view; right, top view. Residues in line form have no effect when mutated on either cAMP production or CLR trafficking (these are not named); residues in stick form alter cAMP production but not CLR trafficking; residues in gray ball and stick form show small to medium effects on CLR trafficking; residues in white ball and stick form show large effects on CLR trafficking. The latter three classes are identified individually.

Table 1: hαCGRP-Stimulated Cyclic AMP Production in RAMP1 Alanine Mutants <sup>a</sup>						
location	mutant	n	pEC <sub>50</sub> (WT)	pEC <sub>50</sub> (mutant) <sup>b</sup>	E <sub>max</sub> (WT)	E <sub>max</sub> (mutant) <sup>b</sup>
helix 1	N31A	3	10.2 ± 0.57	10.6 ± 0.23	76.5 ± 1.35	74.9 ± 3.85
	L35A	3	9.99 ± 0.44	10.6 ± 0.30	72.4 ± 3.02	82.5 ± 2.56
	E38A	3	10.3 ± 0.12	10.6 ± 0.18	72.1 ± 2.74	86.4 ± 1.38**
	L41A	3	10.4 ± 0.20	10.2 ± 0.52	79.7 ± 6.39	72.1 ± 1.20
	T42A	3	10.3 ± 0.14	10.3 ± 0.12	73.8 ± 7.02	81.9 ± 1.96
	Q45A	3	10.1 ± 0.29	10.4 ± 0.31	84.2 ± 5.78	80.3 ± 8.70
	V46A	3	10.4 ± 0.42	10.2 ± 0.53	87.5 ± 2.27	74.6 ± 9.21
	<b>M48A</b>	3	10.6 ± 0.23	10.1 ± 0.29	52.1 ± 9.8	39.5 ± 3.2
	E49A	3	10.4 ± 0.42	10.2 ± 0.53	87.5 ± 2.27	77.1 ± 8.94
	<b>W56A</b>	3	10.8 ± 0.04	10.6 ± 0.17	54.5 ± 10.5	45.2 ± 4.3
loop 1						
helix 2	<b>Y66A</b>	4	10.3 ± 0.32	6.83 ± 0.08	62.2 ± 12.2	20.1 ± 10.5*
	L69A	3	11.0 ± 0.21	10.1 ± 0.21*	73.3 ± 10.4	79.9 ± 7.32
	T73A	3	10.3 ± 0.24	9.26 ± 0.18*	95.1 ± 3.69	69.9 ± 8.41
loop 2	<b>P85A</b>	3	10.1 ± 0.07	7.78 ± 0.1***	59.7 ± 7.2	32.7 ± 4.3*
helix 3	<b>N86A</b>	3	10.3 ± 0.22	9.27 ± 0.2*	70.5 ± 9.5	46.0 ± 8.6
	D90A	3	10.5 ± 0.33	10.3 ± 0.44	83.0 ± 15.7	84.2 ± 4.57
	F93A	3	10.9 ± 0.08	10.2 ± 0.39	71.5 ± 11.5	71.1 ± 6.54
	L94A	3	10.3 ± 0.59	10.7 ± 0.17	58.3 ± 7.99	90.6 ± 1.48*
	<b>H97A</b>	4	10.2 ± 0.25	8.97 ± 0.41*	72.8 ± 9.5	34.3 ± 6.2*
	<b>F101A</b>	4	10.2 ± 0.12	9.81 ± 0.23	63.4 ± 3.67	32.5 ± 3.39***
	<b>D113A</b>	5	10.3 ± 0.21	9.69 ± 0.17*	72.2 ± 7.5	59.6 ± 7.5
	<b>P114A</b>	3	10.5 ± 0.1	9.58 ± 0.16**	69.0 ± 9.8	46.3 ± 12.6
loop 3	<b>P115A</b>	3	10.5 ± 0.1	10.3 ± 0.1	69.0 ± 9.8	65.8 ± 10.7

<sup>a</sup> All RAMP1 mutants were coexpressed with the CLR. Residues in bold are conserved. Y66A pEC<sub>50</sub> is n = 2 values as two others were pEC<sub>50</sub> < 6. Values are expressed as means ± SEM. <sup>b</sup> \*, P < 0.05; \*\*, P < 0.01; \*\*\*, P < 0.001 vs WT by t test.

postulated CGRP binding region (18). By contrast, helix 1 is predicted to have no involvement in CLR receptor function.

A series of alanine mutants were produced to further explore the role of the different portions of RAMP1 (Figure 3). These included the conserved residues M48 (helix 1), W56 (loop 1, between helices 1 and 2), Y66 (helix 2), P85 (loop 2, between helices 2 and 3), N86, H97, F101 (helix 3), and D113, P114, and P115 (loop 3, between helix 3 and the transmembrane domain). In addition, the following residues were mutated to gain further information about the roles of each domain of RAMP1: N31, L35, E38, L41, T42, Q45, V46, and E49 (helix 1, facing outward), L69 and T73 (helix 2), and D90, F93, and L94 (helix 3, facing the hydrophobic patch postulated to be the CLR interaction site).

**Effect of Mutations on cAMP Production.** The WT CGRP receptor was potently activated by CGRP and elevated cAMP to between 50% and 95% of the amount produced by 50

μM forskolin (Table 1, Figure 4). None of the mutants in helix 1 or the loop connecting it with helix 2 decreased cAMP production; E38A marginally increased the maximum response to CGRP. Within helix 2, all three mutants examined (Y66A, L69A, and T73A) impaired production of cAMP. For L69A and T73A the effects were manifested as 10-fold reductions in the potency of CGRP; for Y66A, there was an almost complete loss of responsiveness to CGRP. For helix 3 and the connecting loop to helix 2, P85A, N86A, H97A, and F101A all impaired cAMP production, typically at least halving the maximum response (although this was not significant for N86A) and, for P85A, N86A, and H97A, reducing CGRP potency. By contrast, D90A and F93A did not impair cAMP production; L94A had an increased maximum response. In the connecting loop to the transmembrane helix, both D113A and P114A reduced CGRP potency, but P115A had no significant effect.

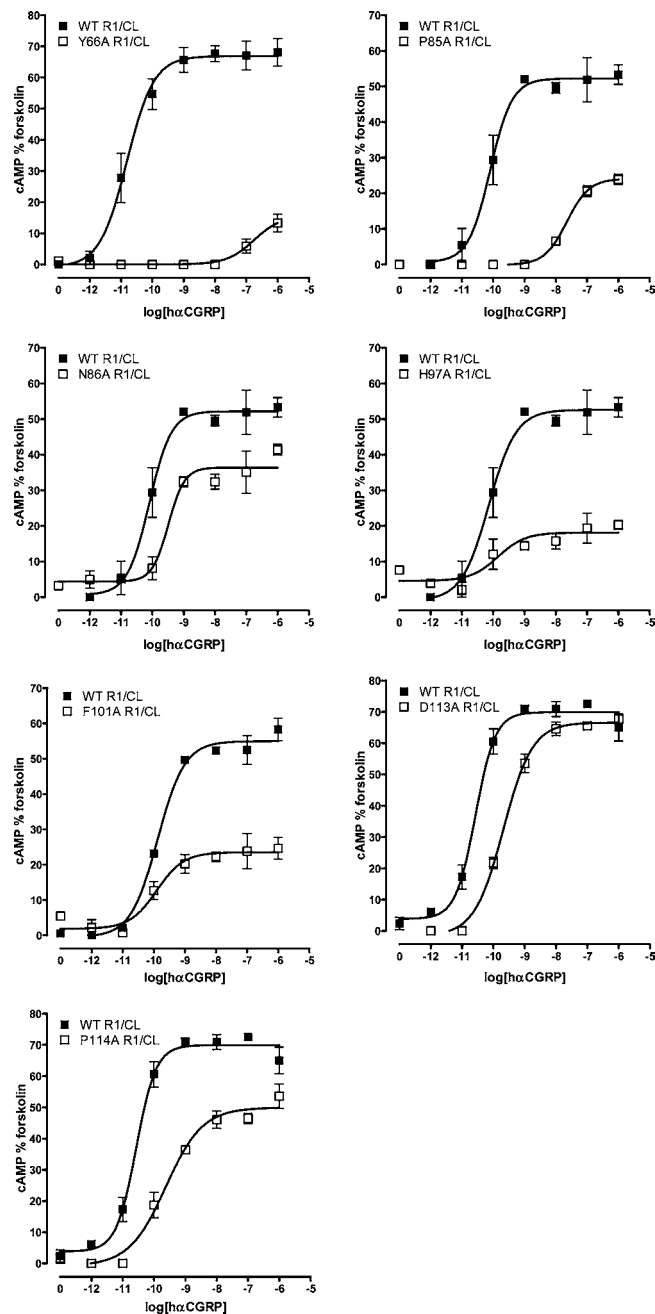


FIGURE 4: Effects of mutations of conserved RAMP1 residues on CGRP-stimulated cAMP production. Figures show representative data from experiments performed at least three times. Points are means  $\pm$  SEM of duplicate determinations.

**Effect of Mutants on RAMP Expression.** RAMP1 lacks an endogenous glycosylation site and has an endoplasmic reticulum retention signal and so is retained intracellularly unless it can complex with a GPCR. CLR is also largely retained intracellularly unless it is coexpressed with a RAMP. Thus the amount of cell surface expression of CLR seen when it is coexpressed with RAMP1 gives a measure of the ability of the two proteins to interact functionally with each other (Figure 5). For comparison, the effects of alanine mutation on the four conserved cysteines which take part in disulfide bonds were also measured. Mutation of these abolishes all responsiveness to CGRP (11, 12, 17). All of the conserved residue mutants, with the exception of W56A and D113A, showed significant reductions in the ability to traffic CLR to the cell surface compared to controls. Y66A

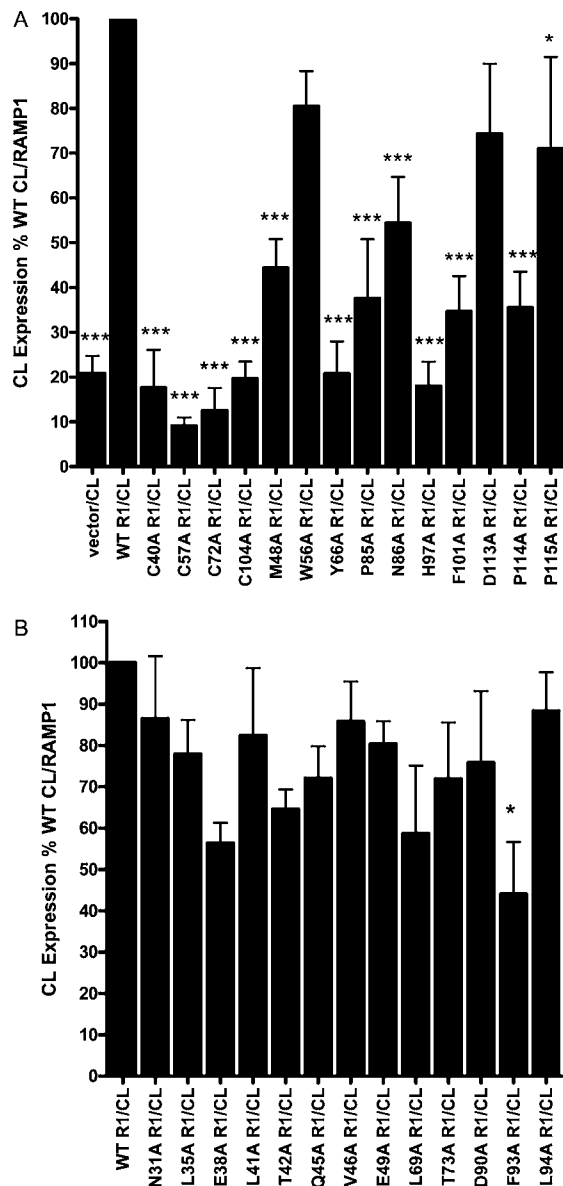


FIGURE 5: Effects of RAMP1 mutations on cell-surface expression of HA-CLR (denoted as CL on figures): (A) conserved residues; (B) other residues.  $N = 3-5$ , each experiment with eight replicates. \*,  $P < 0.05$ ; \*\*\*,  $P < 0.001$  vs WT by one-way ANOVA/Dunnett's.

and H97A both reduced expression of HA-CLR to that seen in the absence of WT RAMP1 and also that with the cysteine to alanine mutations, whereas M48A, P85A, F101A, P114A, and P115A appeared less deleterious. The first four of these reduced cell-surface CLR expression to 30–55% of control and P115A only reduced expression to 70% of control. M48A may have a more deleterious effect on CLR trafficking than appears from these data as it is significantly overexpressed compared to other mutants (see below); however, the mutated RAMP clearly has not suffered a complete loss of ability to recognize CLR. The ability of the nonconserved mutants to traffic CLR to the cell surface was not significantly different from wild type, with the exception of F93A. Due to the poor cell-surface expression of most of the mutants and the likely low affinity of others, no attempt was made to measure  $B_{\max}$  values by radioligand binding.

The total cellular expression of the conserved mutants was examined by Western blotting (Figure 6). The only mutant

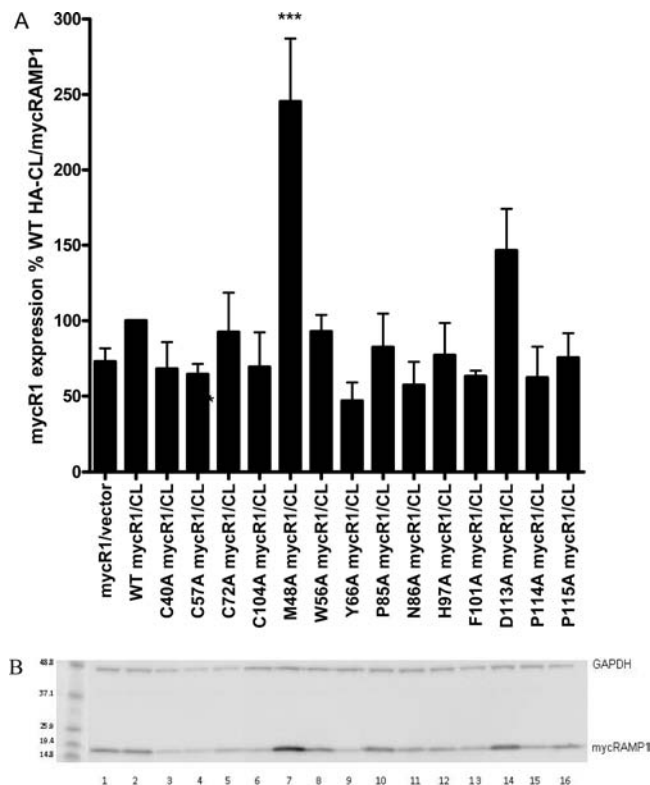


FIGURE 6: Effects of RAMP1 mutations on total cellular expression of myc-RAMP1. (A) Average expression obtained from quantitative Western blotting,  $N = 3$  independent transfections and corresponding Western blots. \*\*\*,  $P < 0.001$  by one-way ANOVA followed by Dunnett's test vs WT. (B) Representative Western blots for each mutant, order of lanes as bars in (A).

that showed a significant change in expression was M48A, where there was 3-fold overexpression compared to wild type. All mutants were produced at the expected molecular weights, suggesting that there were no gross abnormalities during synthesis.

**Effect of M48A and W56A on AM Responsiveness.** The lack of effect of mutation of conserved residues in helix 1 (M48A) and loop 1 (W56A) on CGRP-induced cAMP formation and CLR translocation warranted further interrogation of the importance of these residues. To confirm that the lack of functional perturbation at these positions was not agonist specific, a second agonist of CGRP receptors, AM, was also tested. Consistent with the CGRP data, there were no differences in  $pEC_{50}$  or  $E_{max}$  with either of these mutants. M48A hAM  $pEC_{50}$   $7.95 \pm 0.20$  vs WT  $8.57 \pm 0.20$ ;  $E_{max}$  M48A,  $46.6 \pm 4.06$ , WT  $55.9 \pm 7.64$ , all  $n = 5$ . W56A hAM  $pEC_{50}$   $7.98 \pm 0.54$  vs WT  $8.33 \pm 0.23$ ;  $E_{max}$  W56A  $58.8 \pm 9.00$  vs WT  $57.4 \pm 13.6$ , all  $n = 3$ ,  $\pm$ SEM.

## DISCUSSION

RAMPs interact with GPCRs to modulate their expression at the cell surface, pharmacology, signaling, and intracellular trafficking. However, we have limited understanding of the role of different regions of the RAMP proteins in governing these effects. In particular, the regions of the RAMP extracellular N-terminus which interact with the GPCR and potentially the ligands which act at RAMP/GPCR complexes have not been defined. In this study the function of 23 individual residues in the extracellular domain of RAMP1 has been examined by alanine mutagenesis. In addition, this

domain has been analyzed by two complementary approaches to predict protein–protein interaction sites on the surface of RAMP1. The mutagenesis data demonstrated that the majority of the residues in RAMP1 that alter the ability of CGRP to stimulate cAMP production, either directly or by altering CLR trafficking to the cell surface, are clustered on the second and third helices of RAMP1. By contrast, residues in the first helix, which were predicted to have little effect, generated a WT-like phenotype when mutated to alanine (Figure 2). The modeling analysis also identified the region between helices 2 and 3 as a putative protein–protein interaction site (Figure 2). This has independently been identified as the likely CLR interaction site based on analysis of the crystal structure of RAMP1 (18).

Kusano et al. have identified three significant classes of residues, based on their analysis of the RAMP1 structure (Figure 1): those involved in CLR binding, those involved in CGRP (ie ligand) binding, and those needed for interhelical packing within RAMP1 (18). This classification provides a convenient framework to consider the results of the present study.

The proposed CLR binding site consists of a cluster of residues at the C-terminal end of helix 3, involving F93, H97, and F101. In the present study, mutation of all of these residues reduced CLR association, although there were considerable differences in the functional consequences of alanine substitution at these positions. H97A had the most profound effects, almost completely prohibiting trafficking of CLR to the cell surface; this is likely to explain why it reduced both the potency of CGRP and also the maximum stimulation. F101A produced a less severe disruption of CLR trafficking; in line with this, the mutation did not alter CGRP potency but merely reduced the maximum response. Previously, it was reported by others that H97A showed reasonable expression but reduced CGRP binding but F101A had no effect on binding or expression (13). The differences between the studies are probably related to the cell line used or the different methodologies. F93A had the smallest effect on CGRP receptor function; it impaired presentation of CLR to the cell surface, but this did not result in any reduction in CGRP responsiveness. Kusano et al. (18) note that, in addition to a potential role in CLR binding, the side chain of F93 contributes to stabilizing the interface with helix 1. An F93I substitution, on the other hand, reduced CGRP potency but not CLR expression (16). Therefore, it is possible that F93 has a minor role in CGRP receptor function.

The mutant Y66A had very similar effects to H97A; the protein is still synthesized but does not associate with CLR and so is retained intracellularly. This residue in helix 2 was assigned no specific function by Kusano and colleagues in their analysis of the RAMP1 crystal structure, but it is opposite H97 and its side chain points toward it. Thus both could participate in the putative CLR binding site. Y66 would reinforce the general hydrophobic character of this area. H97 can participate in both hydrophobic and Coulombic interactions; the latter would be strengthened in the hydrophobic environment provided by Y66.

Kusano et al. speculated that the ligand binding site for CGRP could be formed by a cluster of residues at the C-terminal end of helix 2: R67, D71, W74, N78, and W84 (18). The exact way in which this postulated CGRP binding domain functions remains to be established, and its inves-



tigation was not the primary goal of the current study. W74 is important for the binding of the allosteric antagonist BIBN4094BS, but there is no evidence it directly contributes to CGRP binding; however, its equivalent in RAMP3 contributes to high-affinity AM binding (14–16). Thus the evidence is strong that this part of RAMP1 is in close proximity to bound ligands. The mutants L69A and T73A are close to this cluster. Both caused a decrease in  $pEC_{50}$ . In the RAMP1 crystal structure, the side chain of L69A is important in ensuring that helix 2 packs against the other two helices (18). The side chain of T73 hydrogen bonds to the backbone of Ala 70. Neither mutant is likely to cause any gross misfolding of RAMP1 as both can still associate with CLR and reach the cell surface. Their effects may be best explained as an effect on the postulated CGRP interaction site. Both are buried and so are unlikely to be primary ligand contacts; they may stabilize the overall architecture of the ligand binding domain.

A number of mutants may produce their effects in several ways. P85A and N86A both disrupt trafficking of CLR. They are remote from the postulated CLR binding site at the base of helix 3; however, lying on the loop between helices 2 and 3 they may indirectly alter helix packing and so disrupt CLR association. Both also reduced the potency of CGRP; particularly for N86A, the effect on CLR association is so small that it may not fully explain the reduced CGRP sensitivity (M48A causes a greater reduction in CLR trafficking than N86A but has no effect on CGRP potency). As they are close to the proposed CGRP binding site on helix 2, an effect here is more likely to account for the impaired CGRP responsiveness.

As reported previously (13), L94A increases the maximum response seen following CGRP stimulation; this has previously been interpreted as relief of steric hindrance. Kusano et al. note that L94 is on the edge of the proposed CLR interaction site (18); however, L94A does not disrupt CLR trafficking. The residue is not particularly close to the proposed ligand binding site on helix 2, but an effect on CGRP binding rather than CLR association seems most likely. It may act indirectly by altering the conformation of part of CLR that is in contact with CGRP.

D113, P114, and P115 are all outside the area of the current structure of RAMP1, but they would be expected to be on a loop linking the trihelical bundle with its transmembrane domain, on the lower surface of the protein. D113A did not show any significant reduction in expression, although the trend suggested there was a small decrease. It also only demonstrated a marginal (4-fold) decrease in potency. The small size of these effects makes it difficult to resolve the mechanism of its effects, but it is clearly of only minor importance. It may interact with the juxtamembrane region of the CLR. It is tempting to see P114 as preventing secondary structure formation in the polypeptide backbone and maintaining flexibility in the region.

A striking feature of the study was the location of residues which had no effect on CGRP responsiveness. These were chiefly found in the first helix and the loop which links it to the second helix; they include the two conserved residues M48 and W56. L35, L41, M48, and W56 all have been identified as being structurally important in ensuring that helix 1 packs against helix 3 (18). The mutant M48A showed a reduced ability to traffic CLR to the cell surface (although

paradoxically increasing the total amount of RAMP1 present within the cell), consistent with some role in maintaining the CLR binding site. It is well placed to buttress the putative site identified by Kusano et al. (18). It appears that none of the other residues are individually crucial for the functioning of the CGRP receptor. This raises questions as to the function of W56; it is a conserved residue, in close proximity to the putative CLR binding site so its lack of effect is surprising. Given that RAMPs interact with a range of other GPCRs (5, 6), it may be required for interactions with one or more of these. Overall, the data strongly suggest that helix 1 plays a lesser role than helices 2 and 3 in association with CLR and CGRP binding. This in turn reinforces the belief that the predicted second and third helices on RAMP1 are responsible for these functions.

The study has also allowed an evaluation of the predicted structure of RAMP1 against that determined experimentally (17, 18). The two are in very close agreement; indeed, the mutants assessed in this study were made on the basis of the model before the crystal structure became available. Thus the *ab initio* approach used to generate the model may be of general utility.

In summary, the current study suggests important roles for a number of residues within helices 2 and 3 of RAMP1. There is broad support for distinct CLR and CGRP recognition domains formed by these two helices. H97 and Y66 are particularly important for CLR association. Other residues in their vicinity play lesser roles in these functions. L69 and T73 have a role, possibly indirect, in CGRP recognition. Helix 1 appears to play only an indirect role in forming a CGRP receptor. It will be particularly interesting to see if other RAMP-interacting GPCRs and their ligands use different parts of the RAMP1 structure.

## SUPPORTING INFORMATION AVAILABLE

Figures S1 and S2 showing a superimposition of the crystal structure and model of RAMP1. This material is available free of charge via the Internet at <http://pubs.acs.org>.

## REFERENCES

1. McLatchie, L. M., Fraser, N. J., Main, M. J., Wise, A., Brown, J., Thompson, N., Solari, R., Lee, M. G., and Foord, S. M. (1998) RAMPs regulate the transport and ligand specificity of the calcitonin-receptor-like receptor. *Nature* 393, 333–339.
2. Muff, R., Buhlmann, N., Fischer, J. A., and Born, W. (1999) An amylin receptor is revealed following co-transfection of a calcitonin receptor with receptor activity modifying proteins-1 or -3. *Endocrinology* 140, 2924–2927.
3. Christopoulos, G., Perry, K. J., Morfis, M., Tilakaratne, N., Gao, Y., Fraser, N. J., Main, M. J., Foord, S. M., and Sexton, P. M. (1999) Multiple amylin receptors arise from receptor activity-modifying protein interaction with the calcitonin receptor gene product. *Mol. Pharmacol.* 56, 235–242.
4. Hay, D. L., Poyner, D. R., and Sexton, P. M. (2006) GPCR modulation by RAMPs. *Pharmacol. Ther.* 109, 173–197.
5. Bouschet, T., Martin, S., and Henley, J. M. (2005) Receptor-activity-modifying proteins are required for forward trafficking of the calcium-sensing receptor to the plasma membrane. *J. Cell Sci.* 118, 4709–4720.
6. Christopoulos, A., Christopoulos, G., Morfis, M., Udawela, M., Laburthe, M., Couvineau, A., Kuwasako, K., Tilakaratne, N., and Sexton, P. M. (2003) Novel receptor partners and function of receptor activity-modifying proteins. *J. Biol. Chem.* 278, 3293–3297.
7. Zumpe, E. T., Tilakaratne, N., Fraser, N. J., Christopoulos, G., Foord, S. M., and Sexton, P. M. (2000) Multiple ramp domains are required for generation of amylin receptor phenotype from the

- calcitonin receptor gene product. *Biochem. Biophys. Res. Commun.* 267, 368–372.
8. Fraser, N. J., Wise, A., Brown, J., McLatchie, L. M., Main, M. J., and Foord, S. M. (1999) The amino terminus of receptor activity modifying proteins is a critical determinant of glycosylation state and ligand binding of calcitonin receptor-like receptor. *Mol. Pharmacol.* 55, 1054–1059.
9. Fitzsimmons, T. J., Zhao, X., and Wank, S. A. (2003) The extracellular domain of receptor activity-modifying protein 1 is sufficient for calcitonin receptor-like receptor function. *J. Biol. Chem.* 278, 14313–14320.
10. Hoare, S. R. (2005) Mechanisms of peptide and nonpeptide ligand binding to class B G-protein-coupled receptors. *Drug Discov. Today* 10, 417–427.
11. Steiner, S., Born, W., Fischer, J. A., and Muff, R. (2003) The function of conserved cysteine residues in the extracellular domain of human receptor-activity-modifying protein. *FEBS Lett.* 555, 285–290.
12. Flahaut, M., Pfister, C., Rossier, B. C., and Firsov, D. (2003) N-Glycosylation and conserved cysteine residues in RAMP3 play a critical role for the functional expression of CRLR/RAMP3 adrenomedullin receptor. *Biochemistry* 42, 10333–10341.
13. Kuwasako, K., Kitamura, K., Nagoshi, Y., Cao, Y. N., and Eto, T. (2003) Identification of the human receptor activity-modifying protein 1 domains responsible for agonist binding specificity. *J. Biol. Chem.* 278, 22623–22630.
14. Mallee, J. J., Salvatore, C. A., LeBourdelle, B., Oliver, K. R., Longmore, J., Koblan, K. S., and Kane, S. A. (2002) Receptor activity-modifying protein 1 determines the species selectivity of non-peptide CGRP receptor antagonists. *J. Biol. Chem.* 277, 14294–14298.
15. Hay, D. L., Christopoulos, G., Christopoulos, A., and Sexton, P. M. (2006) Determinants of 1-piperidinecarboxamide, N-[2-[[5-amino-1-[[4-(4-pyridinyl)-1-piperazinyl]carbonyl]pentyl]amino]-1-[(3,5-dibromo-4-hydroxyphenyl)methyl]-2-oxoethyl]-4-(1,4-dihydro-2-oxo-3(2H)-quinazolinyl)] (BIBN4096BS) affinity for calcitonin gene-related peptide and amylin receptors—the role of receptor activity modifying protein 1. *Mol. Pharmacol.* 70, 1984–1991.
16. Qi, T., Christopoulos, G., Bailey, R. J., Christopoulos, A., Sexton, P. M., and Hay, D. L. (2008) Identification of N-terminal receptor activity-modifying protein residues important for calcitonin gene-related peptide, adrenomedullin, and amylin receptor function. *Mol. Pharmacol.* 74, 1059–1071.
17. Simms, J., Hay, D. L., Wheatley, M., and Poyner, D. R. (2006) Characterization of the structure of RAMP1 by mutagenesis and molecular modelling. *Biophys. J.* 91, 662–669.
18. Kusano, S., Kukimoto-Niino, M., Akasaka, R., Toyama, M., Terada, T., Shirouzu, M., Shindo, T., and Yokoyama, S. (2008) Crystal structure of the human receptor activity-modifying protein 1 extracellular domain. *Protein Sci.* (in press).
19. Bailey, R. J., and Hay, D. L. (2006) Pharmacology of the human CGRP1 receptor in Cos 7 cells. *Peptides* 27, 1367–1375.
20. Bailey, R. J., and Hay, D. L. (2007) Agonist-dependent consequences of proline to alanine substitution in the transmembrane helices of the calcitonin receptor. *Br. J. Pharmacol.* 151, 678–687.
21. Glaser, F., Pupko, T., Paz, I., Bell, R. E., Bechor-Shental, D., Martz, E., and Ben-Tal, N. (2003) ConSurf: identification of functional regions in proteins by surface-mapping of phylogenetic information. *Bioinformatics* 19, 163–164.
22. Fernandez-Recio, J., Totrov, M., Skorodumov, C., and Abagyan, R. (2005) Optimal docking area: a new method for predicting protein-protein interaction sites. *Proteins* 58, 134–143.

BI801869N